Research Article Adv. Mater. Lett. 2016, **7**(9), 760-764 Advanced Materials *Letters*

www.vbripress.com/aml, DOI: 10.5185/amlett.2016.6077

Mesoporous silica polymer nanocomposites functionalized with vinyl pyridine and vinyl pyrrolidinone for the adsorption of humic acid

G. Robin Wilson, Amit Dubey*

Department of Chemistry, Maulana Azad National Institute of Technology (MANIT), Bhopal 462051, M.P, India

*Corresponding author. E-mail: dramit.dubey@gmail.com

Received: 31 July 2015, Revised: 12 February 2016 and Accepted: 25 May 2016

ABSTRACT

In order to induce the hydrophobicity and the influence of functional vinyl monomers, vinyl pyridine (VP), vinylpyrolidinone (V2P) and vinylsulphonic acid (VSA) were impregnated into SBA-15 matrix to generate SBA/L nanocomposites and characterized for the adsorption of humic acid (HA) for the first time. The structural order of the SBA/L samples was confirmed by standard physicochemical characterizations (powder X-ray diffraction (PXRD), adsorption isotherm, SEM etc.). Considerable adsorption (120-140 mg/g) of HA was observed over basic (SBA/VP and SBA/V2P) nanocomposites compared to the acidic ones. Adsorption parameters like effect of temperature, pH, weight of the adsorbent and time were studied. The possible mechanistic pathway for hydrophilic/hydrophobic interactions was also explained. Copyright © 2016 VBRI Press.

Keywords: Vinyl monomer; humic acid; SBA-15/L; adsorption of HA.

Introduction

Mesoporous templates are getting tremendous attention in material science and catalysis due to their enhanced structural properties for many applications. Specifically, the textural properties (surface area, pore size and pore volume) of these porous materials offer notable benefits for catalytic, adsorption, sensors and ion exchange applications [**1-5**]**.** The textural features of these materials may be tailored/altered easily via direct or post functionalization methods. In order to generate the siliceous polymeric nanocomposites, impregnation of polymers directly into the porous templates were already reported but either the long range ordered structure of the silica template could not be retained or the materials lost their porosity [**6-8**]. In perpetuation, we have also reported the synthesis of vinyl monomers functionalized silica polymer nanocomposites for adsorption and catalytic conversions [**9-13**]. Particularly, adsorption of hazardous metal ions and precarious toxic agents on heterogeneous surface is a challenging area for their improved adsorption capacities and repeated utilization [**9**]. Humic acid (HA) largely exists as a macromolecular organic compound in soil, surface water, ground water and is formed by the bio deterioration of plants, animals etc. [**14-16**]. HA is not a single acid molecule but behaves as a mixture of dibasic or infrequently tribasic acid because of phenolic and acidic groups. Therefore, measures should be taken to minimize the existence of HA due to its inimical effect on the human health and the generation of the malignant products in chlorine treated waters [**14, 17-19**]. Ddiversified methods like adsorption, precipitation, oxidation, ion-exchange and osmosis process have been implemented to minimize the percentage of HA in drinking water [**15**]. However, the presence of active functional groups (phenolic or carboxylic acid) of HA in aqueous medium makes it more flexible to alter their chemical properties. Among all, adsorption is considered as one of the most promising methods because of its simpler experimental setup and high capacity to remove HA from aqueous solution [**20**]. Initially, microporous carbons and activated charcoal cloths were employed for the adsorption of HA but because of smaller pore size of microporous carbon, HA molecules were not accessible for adsorption [**21**]. Therefore, the adsorption of HA by mesoporous activated carbons are considered to be the best adsorbents for the removal of HA. In continuation, the adsorption of HA from aqueous solution on magnetic chitosan nanoparticle, anion-exchanged Fe_3O_4 on magnetic mesoporous composite microspheres, surfactant-modified chitosan/zeolite composites and aminopropyl functionalized SBA-15 have also been reported recently [**15, 19, 22-24**]. However, the adsorption of HA over acidic/basic vinyl monomers functionalized SBA-15 material has not been examined. Hence, the present studies deal with the adsorption of HA on silica polymer nanocomposites (SBA/L).

Experimental

Synthesis of SBA/Lxy (where L= VP, V2P and VSA)

The synthesis of mesoporous silica (SBA-15) was carried out similar to the earlier methods [**3**]. Vinyl pyridine (VP), vinyl-2-pyrrolidinone (V2P) and vinyl sulfonic acid (VSA) were chosen to modify the surface properties. For, SBA/VP91 synthesis, calculated amount of styrene (0.21 g), divinyl benzene (0.07 g), VP (0.023 g) and radical initiator (a, a'-azoisobutyronitrile (0.02g), AIBN) were impregnated into 1 g of SBA-15 material using dichloromethane as a solvent at 298 K. The impregnated mixture was dried at 313 K to remove the solvent. The residual solvent and air were removed by keeping the sample mixture in freeze vacuum thaw. The solid mixture was packed in a pyrex tube for polymerization at different intervals of temperature (318 K for 24 h, 333 K for 4 h, 373 K, 393 K and 423 K for 1 h). The sample was dried at 353 K after washing with ethanol. SBA/VP, SBA/V2P and SBA/VSA nanocomposites with different amount of monomers were also prepared keeping identical synthetic conditions (**Table 1**). The products were denoted as SBA/Lxy, where, L represents the ligand and x, y represents the molar ratio of styrene and the ligand (VP, V2P, VSA etc.) respectively.

Table 1. Amount of different monomers for the synthesis of SBA/Lxy nanocomposites (for 1g SBA-15 with 30wt% of polymers).

SBA/VP					SBA/V2P				
^{a}Samples	Sty (g)	DVB (g)	VP (g)	AIBN (g)	^{a}Samples	Sty (g)	DVB (g)	V2P (g)	AIBN (g)
91	0.21	0.07	0.023	0.02	91	0.20	0.07	0.024	0.02
82	0.19	0.07	0.046	0.02	82	0.18	0.07	0.048	0.02
64	0.13	0.07	0.092	0.02	64	0.12	0.07	0.096	0.02

*Represents the % age of styrene and ligand.

Procedure for adsorption of HA

Different amount of adsorbents (100-1000 mg) and 50 ml of HA solution were mixed in a flask fitted with septum for adsorption studies. The solution was kept at 298 K with stirring conditions. The samples were taken periodically using syringe filters and analyzed by UV spectrophotometer at 254 nm. The amount of quantity adsorbed was determined using the following formula Ae = (C_0- Ce) V/M [**19**], where Ae = equilibrium adsorption amount, C_0 = initial HA concentration, Ce = equilibrium concentration, V = volume of HA solution, M = the mass of the adsorbent.

Results and discussion

The PXRD was measured by Hecus X-Ray Systems S3 Model with Cu Kα radiation (k = 1.5404 A) at low angle (0-5^o). Micromeritics ASAP 2020 analyzer was used to study the adsorption isotherms at 83K. The surface area and the pore size distribution were calculated by BET and Barrett–Joyner–Halenda (BJH) method respectively. The diffraction pattern of all the materials (**Fig. 1**) displayed peaks at (100), (110) and (200) planes identical to the SBA-15 [**3**]. Indexing of the diffracted peaks may be ascribed to 2D hexagonal p6mm symmetry confirming the retention of mesoporous nature of SBA/Lxy samples. However, the intensity of the base peak of SBA/Lxy was reduced with the increasing weight of the monomers in comparison to SBA-15. The mesoporous structural order of the SBA/L was maintained up to the styrene: vinyl monomer of 6:4 and then destroyed completely with further addition of the monomers. According to the IUPAC classification, SBA/Lxy (**Fig. 2**) displayed type IV isotherm with H1 hysteresis loop identical to the SBA-15 [**3**]. The small alteration in the shapes of the isotherms may be attributed to the excess stress caused while polymerizing the monomers into the SBA-15 matrix. Pore size distribution curve showed the most of the pores were confined within 30nm **(Fig. 3)**.

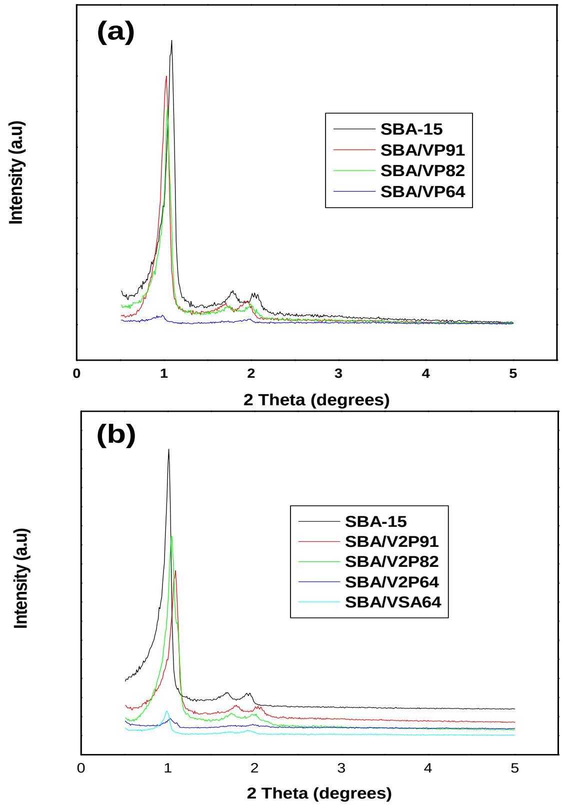

Fig. 1. PXRD pattern of (a) SBA/VP and (b) SBA/V2P& SBA/VSA nanocomposites.

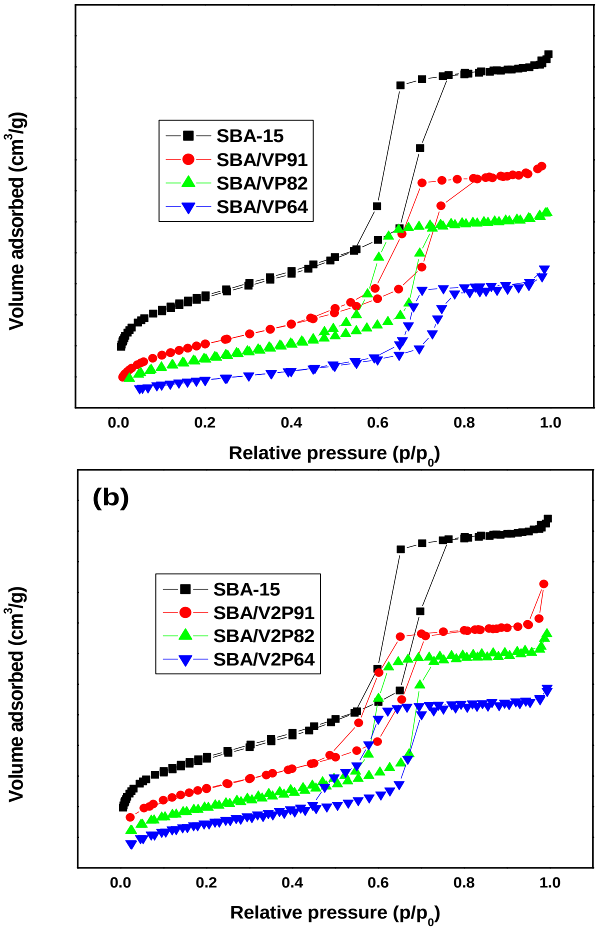

Fig. 2. N_2 Adsorption – desorption isotherms of (a) SBA/VP (b) SBA/V2P nanocomposites.

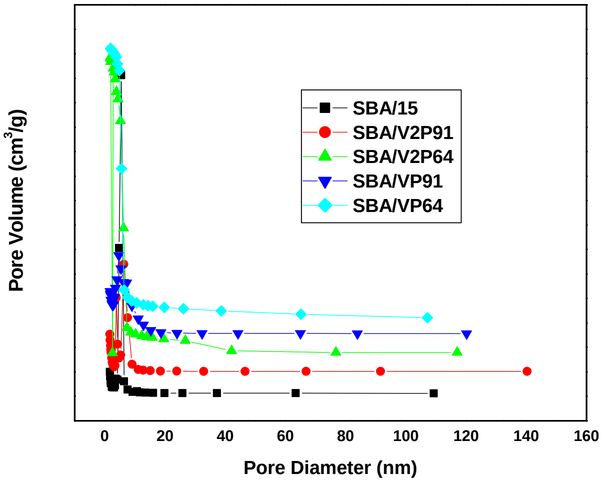

Fig. 3. Pore size distribution curve of SBA and SBA/Lxy nanocomposite.

Surface properties **(Table 2)** of SBA/L were lowered compared to SBA-15 material confirming the polymerization of the ligands on the SBA-15 surface. Scanning electron microscopic studies **(Fig. 4)** revealed the retention of rod like structure of SBA/L nanocomposites. However, small cumulation on the surface was observed after the adsorption of HA and can be due to the ionic interactions between the polymeric surface and HA molecules.

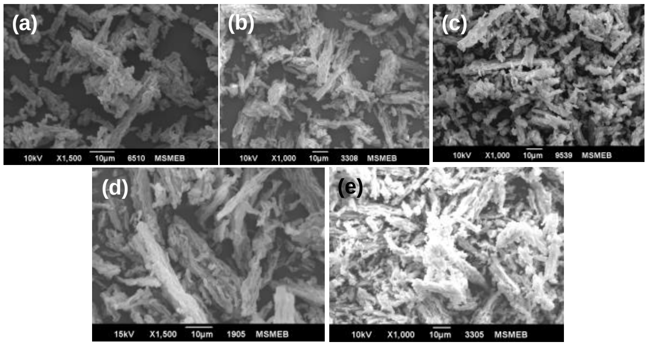

Fig. 4. Scanning Electron Microscopic images of (a) SBA-15 (b) SBA/VP (c) SBA/VP/HA (d) SBA/V2P and (e) SBA/V2P/HA.

Table 2. Structural parameters of different nanocomposites.

Sample		Surface Area (m^2/g)	Pore volume (cm^3/g)	Pore size(nm)	Adsorption (m/g)
SBA-15		653	0.93	7.71	8.1
SBA/V2P	91	379	0.58	6.20	40.6
	82	297	0.44	5.98	55.8
	64	267	0.38	5.75	84.2
SBA/VP	91	448	0.76	6.36	72.9
	82	327	0.51	6.23	81.1
	64	247	0.46	4.41	126.8

Variation of adsorption on (SBA/Lxy)

Variation of adsorption on SBA/Lxy (**Table-2**) showed that very high adsorption of HA (60-140mg/g) was observed on basic adsorbents (SBA/VP & SBA/V2P) compared to acidic (SBA/VSA) adsorbent (20 mg/g). The higher adsorption of SBA/VP adsorbents is due to the more basicity compared to SBA/V2P adsorbents. This is opposite to our previous report [**9**], wherein, highest adsorption of bovine serum albumin was observed on acidic containing vinyl monomers. It is also to be noted here that very low adsorption (<10 mg/g) was obtained with SBA-15 adsorbent infers the necessity of desired functional groups for favorable interactions required for the adsorption. Moreover, low adsorption of HA was also observed on the acidic surface of activated carbon [**25**]. All these observations ensure that the hydrophilic/hydrophobic interactions of the HA functional groups with the surface of silica provides suitable interactions for the adsorption **(Fig. 5).** Change in the concentrations of the monomers revealed that the maximum adsorption could be attained with higher concentration of the ligands and therefore the adsorbents SBA/VP64 and SBA/V2P64 were selected for further studies.

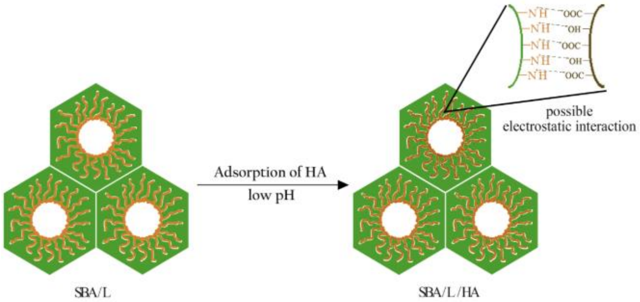

Fig. 5. Mechanistic pathway for probable interactions.

Variation of adsorption time

Influence of the adsorption time **(Fig. 6)** showed that the maximum adsorption was obtained within 3h and became steady afterwards even though the adsorption was allowed for 48h to see the formation of any secondary species/ inter conversion or the repulsion between the adsorbate on the surface. However, the adsorption remained consistent up to 48h infers the stability of the adsorbents and may be helpful in scaling up the process. Therefore, pH- 4 (without adjustment) was chosen for further studies.

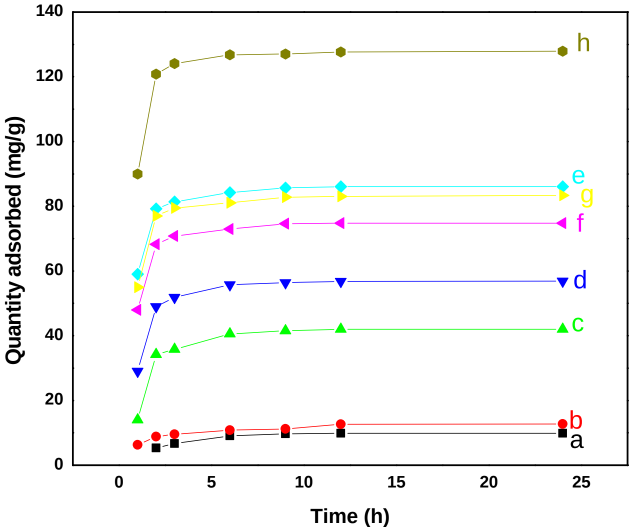

Fig. 6. Effect of the adsorption time on the adsorption of HA over (a) SBA-15, (b) SBA/VSA64, (c) SBA/V2P91, (d) SBA/V2P82, (e) SBA/V2P64, (f) SBA/VP91, (g) SBA/VP82, (h) SBA/VP64 adsorbents.

Variation of the pH on the adsorption of HA

Alteration in the pH (**Fig. 7**) of the solution affirmed that the maximum adsorption (120-140 mg/g) was observed at lower pH (1~4) than at higher pH in both the adsorbents under present experimental conditions. This may be due to the strong electrostatic attractions between the adsorbent and HA (carboxylic or phenolic groups). At higher pH, the basic nitrogen of the VP and V2P acquires more negative charge which results strong electrostatic repulsion with the functional groups of HA thereby reducing the adsorption. However, because of the presence of hydrophobicity on the surface (synergistically), some adsorption was even achieved at higher pH (40-80 mg/g).

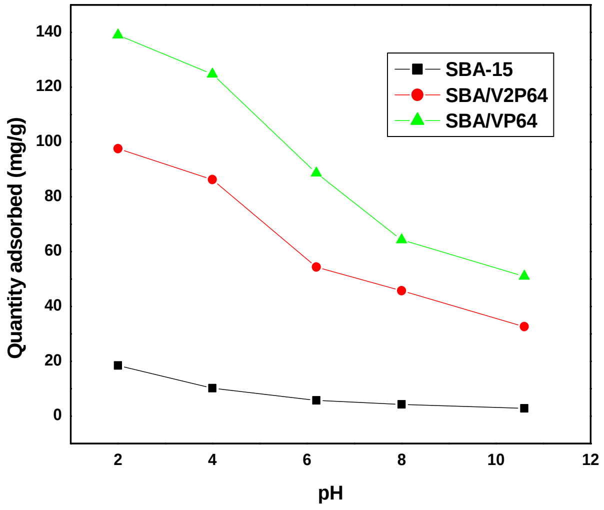

Fig. 7. Effect of pH on adsorption of HA over different adsorbents.

Variation of the temperature on the adsorption of HA

Change in the adsorption temperature **(Fig. 8)** displayed the increasing trend up to 308K and then reduced with further rise in the temperature. This lowering could be due to the reduction in the electrostatic interactions caused by the lesser physisorption rate of the adsorbate on the silica surface.

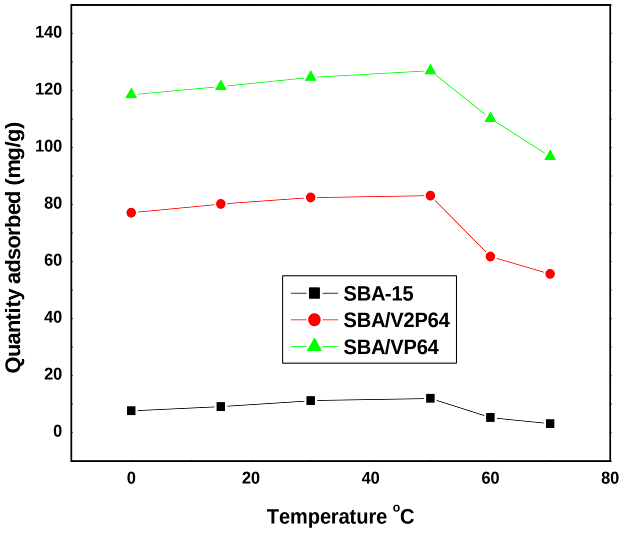

Fig. 8. Effect of temperature on the adsorption of HA.

Effect of the weight of adsorbents

Effect of the weight of the adsorbents **(Fig. 9)** demonstrated that the adsorption increased up to 300mg weight of both the adsorbents but remained constant afterwards. This could be due to the blockage of the adsorption sites available for HA molecules on the adsorbents.

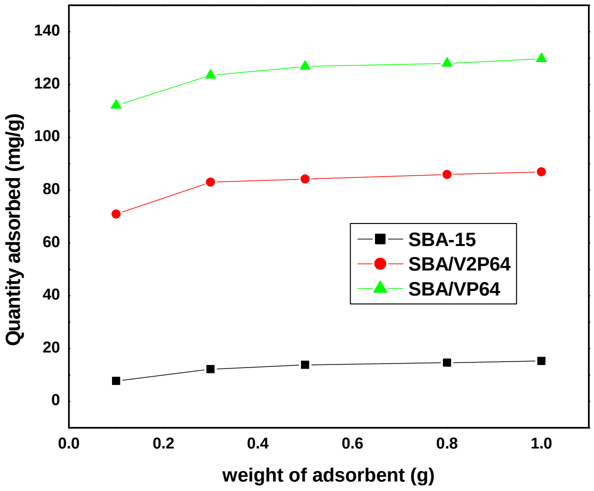

Fig. 9. Effect of weight of adsorbent on the adsorption of HA.

Furthermore, no adsorption was observed with 50mg of the adsorption indicating that the optimum concentration of adsorption sites is essential for the adsorption. To check the recyclability of the adsorbents, SBA/VP64 was filtered and dried after the first batch of adsorption. The adsorption was carried out again with the dried adsorbent. Small variation in the adsorption (7-10%) was achieved after fourth cycle of adsorption indicating that the adsorbents can be recycled and beneficial under environmental friendly conditions.

Conclusion

Ordered mesoporous SBA/L nanocomposites with different concentrations of functional monomers (VP, V2P, and VSA) were synthesized and characterized for the adsorption of HA. Among all, SBA/VP nanocomposites exhibited highest adsorption (140 mg/g) under environmental friendly conditions. The degree of hydrophobicity thus generated on the active surface may lead to different interactions for other hazardous species.

Acknowledgements

AD thanks the institute for research facilities.

References

1. Inagaki, S.; Guan, S.; Fukushima, Y.; Ohsuna, T.; Terasaki, O; *J. Am. Chem. Soc.*, **1999**, *121*, 9611.
   DOI: 10.1021/ja9916658
2. MacLachlan, M.; Asefa, M.; Ozin, G; *Chem. Eur. J.*, **2000**, *6*, 2507.
   DOI: 10.1002/1521
3. Kruk, M.; Jaroniec, M.; Ko, C.; Ryoo, R; *Chem. Mater.*, **2000**, *12*, 1961.
   DOI: 10.1021/cm000164e
4. Molenkamp, W.; Watanabe, M.; Miyata, H.; Tolbert, S; *J. Am. Chem. Soc.*, **2004**, *126*, 4476.
   DOI: 10.1021/ja039296+
5. Wight, A.; Davis, M; *Chem. Rev.*, **2002**, *102*, 3589.
   DOI: 10.1021/cr010334m

6. N. Al-Haq, N.; Ramnauth, R.; Kleinebiekel, S.; Ou, L.; Sullivan, A.; Wilson, J; *Green Chem*. **2002**, *4*, 239.
   DOI: 10.1039/B200806H
7. Cheng, S.; Wang, X.; Chen, S.Y; *Top. Catal*., **2009**, *52*, 681.
   DOI: 10.1007/s11244-009-9216-2
8. Saravanamurugan, S.; Sujandi,.; Han, D.S.; Koo, J.B.; Park, S.E; *Catal. Commun.*, **2008**, *9*, 158.
   DOI: 10.1016/j.catcom.2007.06.002
9. Wilson, G.; Sharma, A.; Srivastava, N.; Sachdev, D.; Dubey, A; *J Porous Mater*., **2015**, *22*, 333.
   DOI: 10.1007/s10934-014-9900-x
10. Wilson, G.; Sharma, A.; Sachdev, D.; Dubey, A; *J Porous Mater*., **2016**, *23*, 195.
    DOI: 10.1007/s10934-015-0070-2
11. Sachdev, D.; Dubey, A.; Wilson, G; *New J. Chem*., **2015**, *39*, 2633.
    DOI: 10.1039/C4NJ01748J
12. Dubey, A.; Choi, M.; Ryoo, M; *Green Chem*., **2006**, *8*, 144.
    DOI: 10.1039/B513845K
13. Sachdev, D.; Dubey, A; *Catal. Commun*., **2013**, *39*, 39.
    DOI: 10.1016/j.catcom.2013.04.016
14. Zhang, X.; Minear, R; *Environ. Sci. Technol*., **2002**, *36*, 4033.
    DOI: 10.1021/es025598k
15. Tana, Y.; Lianga, S.; Yu, S.; Gao, N.; Zhang, J.; Guo, H.; Wang, Y; *Colloids and Surfaces A: Physicochem. Eng. Aspects*., **2012,** *406*, 61.
    DOI: 10.1016/j.colsurfa.2012.04.050
16. Stevenson, F; Humus Chemistry: Genesis, Composition, Reactions; Wiley : USA, **1994**.
    DOI: 978-0-471-59474-1
17. Christman, R.; Ghassemi, M; *J. Am. Water Works Assoc*., **1966**, *58*, 723.
    DOI: JAW_0067669
18. Boorman, G.; Dellarco, V.; Dunnick, J.; Chapin, R.; Hunter, S.; Hauchman, F.; Gardner, H.; Cox, M.; Sills, R; *Envrion. Health Persp*., **1999**, *107*, 207.
    DOI: PMC1566350
19. Tao, Q.; Xu, Z.; Wang, J.; Liu, F.; Wan, H.; Zheng, S; *Micropor. Mesopor. Mat*., **2010**, *131*, 177.
    DOI: 10.1016/j.micromeso.2009.12.018
20. Ngah, W.; Hanafiah, M.; Yong, S; *Colloids Surf. B*., **2008**, *65*, 18.
    DOI: 10.1016/j.colsurfb.2008.02.007
21. Starek, J.; Zukal, A.; Rathousky, J; *Carbon*, **1994**, *32*, 207.
    DOI: 10.1016/0008-6223(94)90184-8
22. Shuang, C.; Wang, M.; Zhou, M.; Zhou, W.; Li, A; *Water. Res*., **2013**, *47*, 6406.
    DOI: 10.1016/j.watres.2013.08.008
23. Dongb, C.; Chena, W.; Liua, C.; Liub, Y.; Liuba, H; *Colloids and Surfaces A: Physicochem. Eng. Aspects*., **2014,** *446*, 179.
    DOI: 10.1016/j.colsurfa.2014.01.069
24. Panda, S.; Mukherjee, M.; De, S; *Journal of Water Process Engineering*, **2015**, *6*, 93.
    DOI: 10.1016/j.jwpe.2015.03.007
25. Karanfil, T.; Kitis, M.; *Environ. Sci. Technol*., **1999**, *33*, 3225.
    DOI: 10.1021/es9810179